Control Engineering Practice 132 (2023) 105429

Contents lists available at ScienceDirect

Control Engineering Practice

journal homepage: www.elsevier.com/locate/conengprac

Optimal management and data-based predictive control of district heating systems: The Novate Milanese experimental case-study

Alessio La Bella [a,*], Ada Del Corno [b]

[a] Dipartimento di Elettronica, Informazione e Bioingegneria, Politecnico di Milano, Via Ponzio 34/5, 20133 Milano, Italy
[b] Dipartimento Tecnologie di Generazione e Materiali, Ricerca Sistema Energetico - RSE S.p.A., Via R. Rubattino 54, 20134 Milano, Italy

ARTICLE INFO

Keywords:
Model predictive control
District heating systems
System identification

ABSTRACT

This paper addresses the modelling and optimal control of district heating systems connected to the electrical grid, with the goal of maximizing their operational efficiency and enabling the participation to electricity markets. Being these systems governed by nonlinear large-scale dynamical models, a novel procedure is proposed, which enables to obtain suitable models for optimization, and consisting in a combination of physical and identified piece-wise linear models. A two-phase optimization and control scheme is then designed, including an offline scheduling problem for participating to the day-ahead energy market, and an online Model Predictive Control system, minimizing the energy consumption of thermal generators while properly satisfying the users thermal demand. The proposed methodology is developed considering a real district heating plant, owned by the energy company A2A S.p.A. and supplying the city of Novate Milanese (Italy), and different experiments on the plant have been carried out. The experimental results and achieved performances are promising, showing a significant reduction of the operational costs and overall gas consumption.

1. Introduction

District Heating Systems (DHSs) are arousing much interest in today energy scenario. The European Commission identified this technology as crucial to meet the 2050 decarbonization targets given its high efficiency (European Commission, 2016). According to the Heat Roadmap Europe project (Paardekooper et al., 2018), DHSs should cover at least 50% of the heating demand of most European countries by 2050, achieving additional 30% of energy savings in the heating sector with respect to 2015. A DHS commonly comprises a heating station for the efficient production of heat, equipped with different thermal generators (e.g. boilers, cogenerators, heat pumps etc.), and a District Heating Network (DHNet) of insulated water pipes, transferring the heat from the heating station to the final users (e.g. buildings). A simple schematic of a DHS is depicted in Fig. 1. In particular, the DHNet is commonly constituted of two parallel layers: a supply layer, where the hot water flow is delivered to users, and a returning layer, where the cold water flowing out from users goes back to thermal generators. Each user is endowed with an internal heat exchanger to absorb the heat delivered by the hot water pipes, which will be then internally used for space heating and/or domestic hot water.

Despite the multiple technical advantages of DHSs, e.g., the possibility of exploiting industrial waste heat or renewable-based technologies (Lake, Rezaie, & Beyerlein, 2017), much research effort is still required from the optimization and control perspective. Being

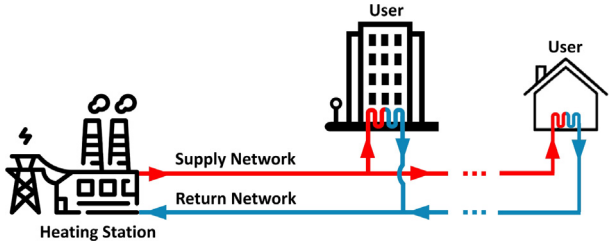

Fig. 1. Schematic of a district heating system.

complex large-scale systems, most DHSs are today operated through basic rule-based control logics, not able to fully exploit their energy efficiency potential, implying that optimization-based control strategies need to be designed (Buffa, Fouladfar, Franchini, Lozano Gabarre, & Andrés Chicote, 2021). Furthermore, a growing interest is arising on the operation of DHSs in synergy with the electrical grid, e.g., managing cogeneration systems or heat pumps for participating to electricity markets (Golmohamadi, Larsen, Jensen, & Hasrat, 2022). In fact, the enhanced thermal inertia and storage capacity of DHSs can be effectively employed to support the electrical system through proper conversion interfaces. Thus, advanced control strategies are needed not

* Corresponding author.
E-mail addresses: alessio.labella@polimi.it (A. La Bella), ada.delcorno@rse-web.it (A. Del Corno).

https://doi.org/10.1016/j.conengprac.2022.105429
Received 30 July 2022; Received in revised form 7 November 2022; Accepted 29 December 2022
Available online 11 January 2023
0967-0661/

only to efficiently satisfy the thermal demand, but also for the optimal participation of the DHS to electricity and flexibility markets.

Nevertheless, this is not a trivial task. A DHS is a large-scale system governed by nonlinear thermo-hydraulics dynamics, e.g., describing the heat propagation in DHNet pipelines, commonly requiring high effort for its modelling and for computing the optimal operation (Sarbu, Mirza, & Crasmareanu, 2019). In this context, this work presents a novel data-based modelling procedure suited for optimization and the design of an effective control strategy for DHSs, based on Model Predictive Control (MPC) methods (Rawlings, Mayne, & Diehl, 2017). The developed control system has been implemented and tested on a real DHS plant, owned by the energy company A2A S.p.A. and located in Italy, enabling to increase its efficiency and to optimally participate to electricity markets.

1.1. Literature review

The detailed modelling of DHSs is described in Machado, Cucuzzella, and Scherpen (2022), in particular analysing stability and passivity properties of nonlinear thermo-hydraulic dynamics. The optimization of DHSs, considering a detailed nonlinear modelling, is formulated in Krug, Mehrmann, and Schmidt (2021), leading to a complex large-scale problem which is solved by assuming a one-step prediction horizon. In fact, the detailed modelling of DHSs involves the presence of many variables and additional states, e.g., representing the temperature gradient along pipes, leading to large-scale complex models not particularly suited for optimization-based controllers (e.g., MPC). This holds not only for the computational effort, but also because these large-scale thermo-hydraulics models require either plenty of measurements to initialize all states (e.g., temperature at each pipe section) or the design of dedicated large-scale nonlinear state estimators (Sandou et al., 2005). To overcome these issues, many MPC regulators proposed in the literature exploit simplified DHS models, where network temperature dynamics are neglected and DHNets are modelled through static power balances (Farahani, Lukszo, Keviczky, De Schutter, & Murray, 2016; Taylor, Long, Marjanovic, & Parisio, 2021; Verrilli, Parisio, & Glielmo, 2016). Relying on this method, a mixed-integer MPC strategy is presented in Verrilli, Srinivasan et al. (2016), enabling to optimize the operations of thermal generators and flexible loads in DHSs. Nevertheless, district heating network temperature dynamics are crucial to be modelled in the control design phase for different reasons, such as: (i) they can describe the DHS thermal inertia given by the presence of long pipelines; (ii) they must be constrained during the operation considering both technical limitations of thermal generators and the proper heat delivery to users substations (e.g., the supply temperature at all users must exceed proper lower bounds to make heat exchangers operate correctly (Krug et al., 2021; Machado, Ferguson, Cucuzzella, & Scherpen, 2023)); (iii) DHNet temperatures can be optimized to minimize heat losses and increase the overall system efficiency (Sandou et al., 2005). Thus, other MPC-based approaches proposed in the literature have considered DHNets temperatures using simplifying modelling assumptions. In Quaggiotto, Vivian, and Zarrella (2021), an MPC system is designed and tested in simulation for a real DHS, modelling only the DHNet returning temperature through a simple linear system. The design of a mixed-integer MPC regulator including average temperature models for each DHNet layer is discussed in Wirtz, Neumaier, Remmen, and Müller (2021), assuming that all users are fed with the same temperature and that the difference between supply and returning temperature is constant. An MPC strategy optimizing DHNet temperatures is presented in Sandou et al. (2005), where the computational effort is reduced assuming constant heat transport delays and fixed DHNet water flow.

As evident from the above-mentioned references, DHNets have been generally modelled with complex nonlinear models (Krug et al., 2021; Machado et al., 2022), with dynamical models relying on simplifications hardly verified in practice (Quaggiotto et al., 2021; Sandou et al., 2005; Wirtz et al., 2021) or with static models relying on power balances (Farahani et al., 2016; Taylor et al., 2021; Verrilli, Parisio, & Glielmo, 2016; Verrilli, Srinivasan et al., 2016). These models are not suited for the design of predictive controllers to optimize DHNet dynamics, e.g., minimizing thermal losses while keeping water temperature at each critical point of the network in prescribed bounds (e.g., supply temperature at each user above a required minimum). There is in fact the necessity of a control-oriented modelling methodology for DHSs which is (i) computationally efficient and (ii) accurately representing the DHNet temperature dynamics, as well as the ones of thermal generators. On the other hand, the mentioned references do not consider the efficient optimization of thermal dynamics in coordination with the participation of DHSs to electricity markets. The latter requires in fact a day-ahead scheduling phase, where the electrical power exchange is defined and communicated to system operators, and an online control phase, where the electrical profile is tracked despite unforeseen load variations (Vasilj, Gros, Jakus, & Zanon, 2017).

1.2. Proposed solution and main contribution

The above discussion motivated the design of a novel modelling and control methodology for DHSs, which main contributions are synthesized in the following.

- *Control-oriented modelling of DHS:* A novel modelling procedure of DHSs is proposed, with the goal of obtaining computational efficient and accurate dynamical models. In particular, the heating station is modelled using mixed-integer physical models. The DHNet thermal dynamics, although nonlinear in nature, are modelled by a piece-wise linear model obtained through a data identification procedure, where different AutoRegressive eXogenous (ARX) systems are learned from operational data for different water flowrate values.
- *Day-ahead optimization and online MPC for DHS:* The proposed DHS dynamical model is then exploited for the design of a two-phase optimization and control procedure. The first, necessary for the participation to the day-ahead energy market, schedules the DHS operations and electrical power profile for the next day considering the load forecasts and the day-ahead energy prices. Then, a *shirking horizon* MPC regulator is designed for the second phase, entitled of real-time tracking the electrical power profile and minimizing DHS gas consumption while properly satisfying the thermal demand. The proposed control system regulates thermal generators operations and the DHNet supply temperature.
- *Experimental setting:* The proposed modelling and control framework has been implemented on a real active DHS plant, located in Novate Milanese (Milan, Italy), owned by the energy company A2A S.p.A.. The company allowed us to perform few days of tests on their own plant, enabling the validation of the identified data-based models and of the performances of the proposed control system. As it will be shown, promising results have been achieved in terms of energy savings and profit maximization, also compared with existing DHS control logics.

A thermal load forecasting algorithm starting from available weather data has been also designed. As it will be discussed, this has been necessary for the day-ahead optimization phase and to perform the real experiments on the plant. This paper extends the preliminary studies reported in La Bella, Del Corno, and Scaburri (2021), where a simplified modelling was considered, the thermal load forecasting and the online MPC control design were missing, and the achieved performances were analysed in simulation.

It is worth noting that, in data-based MPC control approaches, operational data can be used either to learn system dynamics or to directly design model-free controllers (Hewing, Wabersich, Menner, & Zeilinger, 2020). The proposed solution belongs to the first category, as

the DHNet dynamical model is derived using a data-based identification procedure.

The main advantages of the proposed modelling and control solution with respect to the existing approaches are listed in the following. First, the proposed control-oriented modelling enables to accurately represent the real DHS thermal dynamics at each point of interest, as evident from plant experiments, and, moreover, it requires few variables to be measured to initialize the derived models, facilitating the control implementation in a real context. On the other hand, the proposed data-based DHNet modelling procedure, where a piece-wise ARX model is learned instead of relying in an overall nonlinear model, is computationally efficient. In fact, the overall DHS model eventually results in a Mixed-Integer Linear Problem (MILP) efficiently solvable by common solvers, as shown in Section 5. Finally, the designed MPC-based strategy, optimizing both heating generators and DHNet supply temperatures, enables to achieve significant energy savings and an increased economic profit from the electricity market participation, while respecting the temperature requirements at each DHNet critical point, as witnessed by the experiments on the plant.

1.3. Paper outline

The paper is structured as following. The DHS modelling is presented in Section 2, precisely describing the heating station models in Section 2.1 and the DHNnet identification in Section 2.2. The thermal load forecasting problem is described in Section 3. The day-ahead optimization and the MPC design are presented in Section 4. The experimental case-study and the achieved performances are described in Section 5. Final conclusions are given in Section 6.

2. Modelling and system identification

The DHS is modelled as a dynamical discrete-time system with sampling time $\tau = 30$ min $= 0.5$ h, a suitable choice as thermal DHNet transients are generally slow. The index t is used to indicate the discrete time instant and, considering the overall daily operation, $t \in \mathcal{T} = \{1, \dots, M\}$ where $M = 24\ \text{h}/\tau = 48$. The main variables and parameters used in the following are reported in Table 1. As a convention, the upper and lower bounds of each variable are represented with an upper and lower bar, respectively, e.g. $\overline{P}$ and $\underline{P}$ for the variable P.

It is worth underlying that many different DHS configurations exist, e.g., thermal generators can be either located in a single central heating station or dispersed over the DHNet (Werner, 2022). Here, the configuration resembling the Novate Milanese DHS plant is modelled, constituted of a central heating station and a radial DHNnet (a common scenario for DHS, the same depicted in Fig. 1). The proposed approach can be also extended to other configurations, including the corresponding models and constraints.

2.1. Central heating station modelling

The heating station heats up the water coming from the DHNet returning pipes and pumps it through the supply pipes. It commonly comprises several thermal generators, such as boilers, heat pumps and cogenerators, and, in some cases, thermal storages, which can be connected according to several configurations (e.g. in series, in parallel) and differently operated. A schematic of the Novate central heating station is illustrated in Fig. 2. As evident, this is constituted of two heating stages in series: a cogenerator stage, where a set $\mathcal{N}_c$ of cogenerators, with $|\mathcal{N}_c| = n_c = 2$, are connected in parallel, and a gas boiler stage, where a set $\mathcal{N}_b$ of gas boilers, with $|\mathcal{N}_b| = n_b = 4$, are connected in parallel. In the following, cogenerators and gas boilers are modelled using static equations, as the involved time constants are much lower than the DHNet ones and than the chosen sampling time τ, as witnessed by the experiments.

Table 1
Main optimization variables and parameters.

Symbol	Description
P^e_c, P^{th}_c	Cogenerator electrical and thermal power [W]
$\widetilde{P}^{e,aux}_c$	Cogenerator auxiliary systems electrical power [W]
δ_c	Cogenerator operational status
η^e_c, η^{th}_c	Cogenerator electrical and thermal efficiency
q^g_c, q^w_c	Cogenerator gas and water flows [m^3/s]
T^{out}_c	Cogenerator outlet water temperature [K]
T^{in}_c	Cogenerator inlet water temperature [K]
P^e_b, P^{th}_b	Gas boiler electrical and thermal power [W]
$\widetilde{P}^{e,aux}_b$	Gas boiler auxiliary systems electrical power [W]
$\widetilde{P}^{th}_b$	Gas boiler thermal power threshold [W]
δ_b	Gas boiler operational status
η^{th}_b	Gas boiler thermal efficiency
q^g_b, q^w_b	Gas boiler gas and water flows [m^3/s]
T^{out}_b	Gas boiler outlet water temperature [K]
T^{in}_b	Gas boiler inlet water temperature [K]
H_p	Pump head coefficient [m]
n_p	Pump efficiency
P^{th}_u	Thermal power absorbed by a single user [W]
$P^{th}_{u,tot}$	Thermal power absorbed by all users [W]
T^s, T^r	Supply and return DHNet water temperature [K]
T^u	Supply water temperature at a single user [K]
q^w	DHNet overall water flow [m^3/s]
P^e_{hs}	Overall DHS electrical power exchange [W]
$P^{e,out}_{hs}$	Sold electrical power by the DHS [W]
$P^{e,in}_{hs}$	Bought electrical power by the DHS [W]
ρ^w, ρ^g	Water and gas density [kg/m^3]
c^w_s	Water specific heating coefficient [J/(kg K)]
c^g_{lhv}	Gas lower heating value coefficient [J/kg]
$\pi^{e,b}$	Day-ahead electrical energy buying price [€/Wh]
$\pi^{e,s}$	Day-ahead electrical energy selling price [€/Wh]
$\pi^{e,i}$	Imbalance electrical energy price [€/Wh]
π^g	Gas energy price [€/Wh]

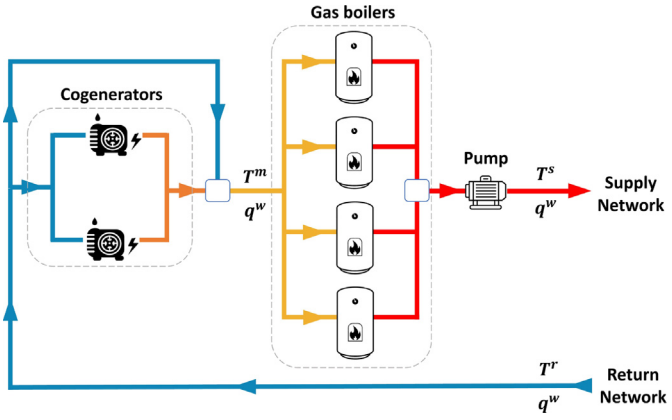

Fig. 2. Schematic of the central heating station of the Novate Milanese plant.

Cogenerators consume gas to produce both electrical and thermal power, consistently with their power capability limits and energy conversion efficiencies. Concerning the electrical production of the ith cogenerator, with $i \in \mathcal{N}_c$, this is

$$P^e_{c,i}(t) = \eta^e_{c,i}\, c^g_{lhv}\, \rho^g\, q^g_{c,i}(t) - \delta_{c,i}(t)\, \widetilde{P}^{e,aux}_{c,i}\,, \tag{1}$$

$$\underline{P}^e_{c,i}\, \delta_{c,i}(t) \le P^e_{c,i}(t) \le \delta_{c,i}(t)\, \overline{P}^e_{c,i}\,, \tag{2}$$

where $\delta_{c,i}(t)$ is a boolean variable indicating if cogenerator i is ON ($\delta_{c,i}(t) = 1$) or OFF ($\delta_{c,i}(t) = 0$), $\eta^e_{c,i}$ is the electrical efficiency, $q^g_{c,i}$ is the consumed gas flow, c^g_{lhv} is the gas lower heating value and ρ^g is the gas density. $\widetilde{P}^{e,aux}_{c,i}$ in (1) represents the electrical power absorbed by the auxiliary systems, modelled with a fixed value estimated by experimental data. The produced thermal power by the ith cogenerator is modelled as

$$P^{th}_{c,i}(t) = \eta^{th}_{c,i}\, c^g_{lhv}\, \rho^g\, q^g_{c,i}(t)\,, \tag{3}$$

with $\eta^{th}_{c,i}$ being the thermal efficiency. The produced thermal power is transferred to the water flowing through the ith cogenerator, implying that

$$P^{th}_{c,i}(t) = c^w_s\, \rho^w\, q^w_{c,i}(t)\, \left(T^{out}_{c,i}(t) - T^{in}_{c,i}(t) \right) . \tag{4}$$

The heat transfer Eq. (4) is based on the steady-flow model, a valid assumption for the chosen sampling time (Cengel, 2002). As evident from Fig. 2, cogenerators are in parallel and their inlet temperature coincides with the one of the DHNet returning layer, i.e.,

$$T^{in}_{c,i}(t) = T^r(t) . \tag{5}$$

Moreover, a fraction of the overall flowing water is not heated up by cogenerators, due to their limited power, but it flows through a bypass. Then, cogenerators water flows, once heated, are mixed in an intermediate collector with the one flowing through the bypass, reaching an overall temperature denoted as $T^m(t)$ (see Fig. 2). This is defined as

$$T^m(t) = \frac{\sum_{i=1}^{n_c} \left(q^w_{c,i}(t) \cdot T^{out}_{c,i}(t) \right) + \left(q^w(t) - \sum_{i=1}^{n_c} q^w_{c,i}(t) \right) \cdot T^r(t)}{q^w(t)} ,$$

which, exploiting (4) and (5), can be simplified as

$$\sum_{i=1}^{n_c} P^{th}_{c,i}(t) = c^w_s\, \rho^w\, q^w(t) \left(T^m(t) - T^r(t) \right) . \tag{6}$$

The thermal power produced by the jth gas boiler, with $j \in \mathcal{N}_b$, is

$$P^{th}_{b,j}(t) = c^w_s\, \rho^w\, q^w_{b,j}(t)\, (T^{out}_{b,j}(t) - T^{in}_{b,j}(t)) , \tag{7}$$

$$\underline{P}^{th}_{b,j}\, \delta_{b,j}(t) \le P^{th}_{b,j}(t) \le \delta_{b,j}(t)\, \overline{P}^{th}_{b,j} , \tag{8}$$

$$P^{th}_{b,j}(t) = \eta^{th}_{b,j}\, c^g_{lhv}\, \rho^g\, q^g_{b,j}(t) , \tag{9}$$

where $\delta_{b,j}(t)$ is a boolean variable indicating if the jth boiler is ON ($\delta_{b,j}(t) = 1$) or OFF ($\delta_{cg,j}(t) = 0$). Gas boilers consume electrical power due to their auxiliary systems, meaning that

$$P^e_{b,j}(t) = -\,\delta_{b,j}(t) \widetilde{P}^{e,aux}_{b,j} . \tag{10}$$

Gas boilers are connected in parallel at the considered plant (see Fig. 2), implying that they are fed with water at the same temperature, i.e.,

$$T^{in}_{b,j}(t) = T^m(t) . \tag{11}$$

After being heated by boilers, the overall water flow is mixed in a final collector and supplied to the DHNet at temperature T^s. As done for cogenerators, the combination of (7) and (11) can be expressed as

$$\sum_{j=1}^{n_b} P^{th}_{b,j}(t) = c^w_s\, \rho^w\, q^w(t)\, (T^s(t) - T^m(t)) . \tag{12}$$

The total DHS electrical power, positive if injected in the main utility, is

$$P^e_{hs}(t) = \sum_{i=1}^{n_c} P^e_{c,i}(t) + \sum_{j=1}^{n_b} P^e_{b,j}(t) - \rho^w\, g\, H_p\, \frac{1}{\eta_p} q^w(t) , \tag{13a}$$

where the last term of Eq. (13a) corresponds to the electrical power consumed by the pump system, where H_p is the pump head coefficient, η_p is the efficiency and g the acceleration gravity. In particular, the experimental tests has shown that the adopted linear model for the pump electrical power provides a good approximation of its real consumption. Let us introduce the boolean variable $\delta^e_{hs}(t)$, where $\delta^e_{hs}(t) = 1$ if, and only if, $P^e_{hs}(t) \ge 0$, and let us introduce $P^{e,out}_{hs}$ and $P^{e,in}_{hs}$ as the produced and absorbed electrical power by the DHS, respectively. Thus, it holds that

$$P^e_{hs}(t) = P^{e,out}_{hs}(t) - P^{e,in}_{hs}(t) , \tag{13b}$$

$$0 \le P^{e,out}_{hs}(t) \le \delta^e_{hs}(t) \overline{P}^e_{hs} , \tag{13c}$$

$$0 \le P^{e,in}_{hs}(t) \le (1 - \delta^e_{hs}(t)) \underline{P}^e_{hs} , \tag{13d}$$

where $\overline{P}^e_{hs} > 0$ and $\underline{P}^e_{hs} < 0$ are the contractual limits for the electrical power exchange with the grid.

At this stage, additional constraints are stated in the following paragraph, specific for the Novate Milanese DHS plant. In fact, not all variables could be externally controlled in the considered plant, as many of them are internally regulated by the local plant controller. This local operation must be also modelled to accurately optimize the plant. Note that the following constraints do not affect the validity of the proposed approach, and they could be either removed or adapted for other DHS case studies.

2.1.1. Local operation of the Novate Milanese heating station

The cogenerators of the Novate Milanese DHS plant are power-controlled, i.e., their electrical power can be imposed and they can be arbitrarily turned ON or OFF. However, their water flow is not controllable, and it is equal either to a constant value $\tilde{q}^w_{c,i}$ (when the ith cogenerator is ON) or zero (when OFF). Thus,

$$q^w_{c,i}(t) = \delta_{c,i}(t)\, \tilde{q}^w_{c,i} . \tag{14}$$

On the other hand, gas boilers are temperature-controlled, i.e., their outlet temperature can be imposed. However, the same outlet temperature must be set for all active gas boilers, which, as evident from Fig. 2, would coincide with the DHNet supply temperature T^s. Thus, it holds that

$$T^{out}_{b,j}(t) = \delta_{b,j}(t)\, T^s(t) . \tag{15}$$

Gas boilers cannot be arbitrarily turned ON, or OFF, since their activation is determined by an internal plant logic. This activates boilers according to a precise sequence (e.g., increasing order with respect to j), so as the number of active boilers is defined by the ratio between their total power request (given by (12)) and a threshold $\widetilde{P}^{th}_b > 0$. To translate this logic in mixed-integer linear constraints, an auxiliary boolean variable δ^M_b is introduced, where $\delta^M_b(t) = 1$ if, and only if, all n_b gas boilers are active at t, i.e.,

$$\sum_{j=1}^{n_b} \delta_{b,j}(t) \ge n_b\, \delta^M_b(t) , \tag{16a}$$

$$\sum_{j=1}^{n_b} \delta_{b,j}(t) \le n_b - 1 + \delta^M_b(t) , \tag{16b}$$

Thus, the boilers' local activation logic can be formulated as

$$\frac{\sum_{j=1}^{n_b} P^{th}_{b,j}(t)}{\widetilde{P}^{th}_b} \ge \sum_{j=1}^{n_b} \delta_{b,j}(t) - 1 , \tag{16c}$$

$$\frac{\sum_{j=1}^{n_b} P^{th}_{b,j}(t)}{\widetilde{P}^{th}_b} \le \sum_{j=1}^{n_b} \delta_{b,j}(t) + \delta^M_b(t) \left(\frac{\sum_{j=1}^{n_b} \overline{P}^{th}_{b,j}}{\widetilde{P}^{th}_b} - n_b \right) , \tag{16d}$$

and

$$\delta_{b,j+1}(t) \le \delta_{b,j}(t), \qquad \forall j \in \{1, \dots, n_b - 1\} , \tag{16e}$$

where the second term on the right-hand side of (16d) serves to maintain feasibility in case all boilers are active.

The thermal power provided by each gas boiler is also regulated by the local plant logic. Precisely, the total power requested to boilers (given by (12)) is automatically distributed among the active ones proportionally to their maximum power. This can be modelled as

$$P^{th}_{b,j}(t) = \frac{\delta_{b,j}(t) \overline{P}^{th}_{b,j}}{\sum_{j=1}^{n_b} \left(\delta_{b,j}(t)\, \overline{P}^{th}_{b,j} \right)} \left(\sum_{j=1}^{n_b} P^{th}_{b,j}(t) \right),$$

which, for the sake of convenience, is rewritten as

$$P^{th}_{b,j}(t) \left(\sum_{j=1}^{n_b} \delta_{b,j}(t)\, \overline{P}^{th}_{b,j} \right) = \delta_{b,j}(t) \overline{P}^{th}_{b,j} \left(\sum_{j=1}^{n_b} P^{th}_{b,j}(t) \right) . \tag{17}$$

Note that the automatic distribution of power uniquely determines the boilers water flow, given the imposed inlet temperature T^m and outlet water temperature T^s, see (7), (11), (15). On the other hand, if a boiler

is OFF, its water flow must be zero. Thus, the following constraint is introduced

$$0 \leq q^w_{b,j}(t) \leq \delta_{b,j}(t)\, Q\,, \tag{18}$$

with $Q \gg 0$ chosen as very large number. In the considered plant, in case all boilers are inactive, the overall water flow is directly supplied to the DHNet through an additional bypass after the cogenerators heating stage, meaning that $T^m = T^s$ as evident from (7).

Remark 2.1. The additional constraints related to the plant internal control logic significantly reduce the feasibility set of the optimization problem, leading to sub-optimal solutions (however satisfying performances are still achieved in the experiments). On the other hand, their introduction may significantly reduce the dimension of the optimization problem. Note that, being cogenerators water flow and inlet temperature imposed, (see (5), (14)), the requested power to cogenerators uniquely determines their outlet water temperature given (4). Moreover, being boilers thermal power, operational status and inlet temperature dictated by the plant internal logic (see (11), (16), (17)), their water flow is uniquely determined once the outlet temperature is imposed, as evident from (7). This implies that inlet/outlet temperatures and water flows of cogenerators and gas boilers can be excluded from the problem formulation, as well as the constraints where these variables appear, considering just thermal and electrical powers. In this case, the heat transfer to the water flow is expressed by (6) and (12), and the single units' temperatures and water flows are a-posteriori computed as the optimal solution is found, leading to a simpler optimization problem to be solved.

2.2. Data-based dynamic modelling of district heating networks

The DHNet is dynamical system, characterized by slow transients for transporting heat along the water pipelines. In particular, only the dynamics of the DHNet temperatures are here modelled, as pressure transients are almost instantaneous with respect to temperatures ones, especially if incompressible fluids are considered (pressure waves travel with the speed of sound in the water, i.e. 1200 m/s, while temperature waves travel with a speed close to the water flow (Benonysson, Bøhm, & Ravn, 1995)). Moreover, as common for different district heating systems, the pump system of the Novate Milanese plant is internally controlled so as DHNet pressure losses are continuously compensated.

Heat propagation in pipes is governed by nonlinear dynamical equations, which modelling as state-space system commonly implies their discretization both in time and in space, introducing different auxiliary state variables (Krug et al., 2021). These models, although fundamental for simulation purposes, are not suited for optimization and control due to their significant non-linearity and the large number of involved variables, hardly measurable in practice. To overcome this issue, it is here proposed to learn suitable DHNet models from the plant operational data, accurately representing the main DHNet thermal dynamics. Before presenting the identified models, some considerations are given to motivate their structure.

Temperatures at different points of the DHNet can be modelled as dynamical systems having as inputs: the supply temperature at the heating station, the total DHNet water flow, the thermal power absorbed of the users, and the ground temperature (DHNet pipes are buried underground). Indicating as $\mathcal{N}_L$ the set of thermal users distributed in the DHNet, a generic DHNnet temperature model can be formulated as

$$T(t) = f\left(\, x(t-1),\, T^s(t),\, q^w(t),\, P^{th}_{u,\forall j\in\mathcal{N}_L}(t), T^{grd}(t)\,\right). \tag{19}$$

The variable x in (19) is introduced to represent a generic vector of internal states of the dynamical temperature model. In fact, the precise definition of the states depend on the selected model structure, that is clarified in the following. In fact, few simplification steps are now performed to Eq. (19) so as to obtain a suitable identification model structure. First of all, the ground temperature is $T^{grd}(t)$ is assumed a constant parameter, and therefore it is removed from the input variables. Then, it is worth noting that thermal equations in water pipes can be considered linear when the flow is fixed (Krug et al., 2021). Inspired by Rathod et al. (2019), this property is exploited to formulate the DHNet model as a piece-wise linear model. To do that, the total DHNet water flow is modelled to take a finite number of n_q values, i.e. $q^w(t) \in \left\{\, \tilde{q}^w_1,\, \ldots,\, \tilde{q}^w_{n_q} \,\right\}$. This can be modelled by stating that

$$q^w(t) = \sum_{k=1}^{n_q} \delta_{q,k}(t)\, \tilde{q}^w_k\,, \qquad \sum_{k=1}^{n_q} \delta_{q,k}(t) = 1\,, \tag{20}$$

where $\delta_{q,k}$ is a boolean variable, equal to 1 if the kth flow level is selected. This enables to formulate (19) as a piece-wise model, i.e.,

$$T(t) = \begin{cases} f_1(x(t-1),\, T^s(t),\, P^{th}_{u,\forall j\in\mathcal{N}_L}(t),\, \tilde{q}^w_1) & \text{if } \delta_{q,1}(t) = 1, \\ \vdots & \\ f_{n_q}(x(t-1),\, T^s(t),\, P^{th}_{u,\forall j\in\mathcal{N}_L}(t),\, \tilde{q}^w_{n_q}) & \text{if } \delta_{q,n_q}(t) = 1, \end{cases} \tag{21}$$

where each function f_k is identified with a linear model structure, representing the temperature at a generic DHNet point when the water flow is $\tilde{q}^w_k$. The water flow levels $\left\{\, \tilde{q}^w_1,\, \ldots,\, \tilde{q}^w_{n_q} \,\right\}$ can be selected exploiting real plant data, so as to comprise the whole operational range with proper resolution, as well as typical water flow values measured at the plant. In case this knowledge is not available, automatic procedures are available, e.g., Breschi, Piga, and Bemporad (2016).

A further simplification must be introduced, due to a limitation of our specific case-study. Indeed, for the considered DHS plant, it was not possible to measure users' thermal power absorption in real-time. Thus, model (21) is modified to take as input the total thermal demand $P^{th}_{u,tot}(t) = \sum_{\forall j\in\mathcal{N}_L} P^{th}_{u,j}(t)$. This, although still not measurable, can be accurately forecasted from weather data through a simple machine learning algorithm, as it will be described in Section 3. Therefore, Eq. (21) is reformulated as

$$T(t) = \begin{cases} f_1(x(t-1),\, T^s(t),\, P^{th}_{u,tot}(t),\, \tilde{q}^w_1) & \text{if } \delta_{q,1}(t) = 1, \\ \vdots & \\ f_{n_q}(x(t-1),\, T^s(t),\, P^{th}_{u,tot}(t),\, \tilde{q}^w_{n_q}) & \text{if } \delta_{q,n_q}(t) = 1. \end{cases}$$

Among the possible linear model structures to learn functions f_k from DHS operational data, ARX models provided very good results. Furthermore, ARX model outputs just depend on past outputs and inputs, which are always measurable, and not on auxiliary internal states, therefore avoiding the necessity of implementing state observers on the plant (Ljung & Glad, 1994).

It is also important to note that just temperature models for few specific points of the DHNet are necessary to properly optimize the considered DHS. These are: (i) the supply temperatures at users' substations, which must be always greater than a lower bound, and (ii) the DHNet return temperature $T^r(t)$, as it must be also bounded and it is necessary to compute the thermal power transferred by the central station (see Section 2.1). Moreover, as it will be evident from the experiments, it is sufficient to model the supply temperature of just few critical users in the DHNet, e.g., the more distant ones from the heating station, being them characterized by the lowest supply temperatures. Defining with $\widetilde{L} \subseteq \mathcal{N}_L$ the subset of identified DHNet users, the following piece-wise linear ARX model is therefore stated, with $j \in \widetilde{L}$,

$$\begin{aligned} T^u_j(t+1) = \sum_{k=1}^{n_q} \delta_{q,k}(t) \Bigg(& \sum_{i=0}^{n^u_\alpha} \alpha^u_{k,i,j}\, T^u_j(t-i) + \\ & + \sum_{i=0}^{n^u_\beta} \beta^u_{k,i,j}\, T^s(t-i) \;+\; \sum_{i=0}^{n^u_\gamma} \gamma^u_{k,i,j}\, P^{th}_{u,tot}(t-i) \Bigg), \end{aligned} \tag{22}$$

where, if kth water flow level is selected, i.e., $q^w(t) = \tilde{q}^w_k$, the kth ARX model is activated to describe the T^u_j dynamics.

The same model structure is used for the DHNet return temperature, i.e.,

$$T^r(t+1) = \sum_{k=1}^{n_q} \delta_{q,k}(t) \left(\sum_{i=0}^{n_\alpha^r} \alpha_{k,i}^r \, T^r(t-i) + \sum_{i=0}^{n_\beta^r} \beta_{k,i}^r \, T^s(t-i) + \sum_{i=0}^{n_\gamma^r} \gamma_{k,i}^r \, P_{u,tot}^{th}(t-i) \right). \tag{23}$$

The terms n_α^u, n_β^u, n_γ^u, n_α^r, n_β^r, n_γ^r in (22), (23) are the ARX model orders, while $\alpha_{k,i,j}^u$, $\beta_{k,i,j}^u$, $\gamma_{k,i,j}^u$, $\alpha_{k,i}^r$, $\beta_{k,i}^r$, $\gamma_{k,i}^r$ are the ARX parameters, which have been estimated from data solving a *Least Squares problem* (Ljung & Glad, 1994). Note that models (22) and (23) can be formulated as mixed-integer linear equations, using techniques presented in Bemporad and Morari (1999).

Each kth ARX model in (22)–(23) has been independently identified using a different training dataset for each water flow level $\tilde{q}_k^w$, where the supply temperature and the thermal demand are varied to excite the DHNet system. Nevertheless, a real operating DHS, as the Novate Milanese plant, cannot be arbitrarily manipulated to gather meaningful training data as users must be always properly supplied. Therefore, training data has been generated through simulation resembling the real plant operation. In particular, a detailed simulator of the Novate Milanese DHNet has been developed in TRNSYS® (Transient System Simulation Tool), a software environment particularly suited for dynamical thermo-hydraulic systems (Lu et al., 2021). The simulator has been developed using the physical data of the Novate Milanese DHNet, provided by A2A S.p.A., and it revealed to be particularly useful for testing the designed control strategy before the implementation on the plant. Once developed, the simulator has been validated with the real plant operational data, showing to accurately model the DHNet thermal dynamics as reported in Section 5. The piece-wise linear models (22) and (23), identified through the simulated training dataset, have been also validated with the real plant operational data, achieving quite satisfactory performances in representing the DHNet temperature dynamics despite their simple model structure, as it will be shown in Section 5.

Before proceeding to the next sections, the upper and lower bounds of the modelled DHNet temperatures are hereafter presented. These will be included in the formulation of the optimization and control problems, together with system models above described.

2.2.1. Thermal constraints of the district heating network

The DHNet supply temperature of the water flowing out from the central heating station is upper and lower bounded, given the physical limits of thermal generators, i.e.,

$$\underline{T}^s \le T^s(t) \le \overline{T}^s. \tag{24}$$

Concerning final users, as mentioned, the supply water temperature must always exceed a lower bound for the proper operation of heat exchangers in satisfying the thermal demand (Krug et al., 2021; Machado et al., 2023). It follows that

$$T_j^u(t) \ge \underline{T}^u(t), \tag{25}$$

where $j \in \widetilde{L}$, and $\underline{T}^u(t)$ is a time-varying bound commonly lower during night-time, as users use less hot water and most radiators are turned off, and higher during the day.

For the considered plant, during the day, users substations automatically regulate the absorbed water flow through internal valves so that their returning temperatures evolve around predefined references (different among the users). During the night, being most user heat exchangers disconnected, the DHNet return temperature shows large variations, given the low thermal demand which typically soars early in the morning. On the other hand, DHNet return temperature must be always constrained between an upper and lower bound due to the limits of thermal generators. Thus, to take into account this behaviour in the proposed DHNet model, the returning temperature is therefore by proper time-varying upper and lower bounds, i.e.,

$$\underline{T}^r(t) \le T^r(t) \le \overline{T}^r(t), \tag{26}$$

where the bounds are defined so as $\overline{T}^r(t) > \underline{T}^r(t)$ and their difference is small during the day, so as to maintain the return DHNet temperature around an average reference, and it is larger during the night-time, so as to respect the thermal limits.

Finally, the DHNet temperatures at the end of the day should not be lower than the one at the beginning for the correct optimization of the DHS operation. To consider this aspect, the following constraints are also included

$$T^r(1) \le T^r(M), \qquad T^s(1) \le T^s(M), \tag{27}$$

where it is recalled that M is the last time instant in the time horizon $\mathcal{T}$.

Remark 2.2. During the implementation on the real plant, (24)–(27) were defined as *soft constraints*, i.e., relaxed through the use of slack variables, to always ensure problem feasibility. Their modelling as relaxed soft constraints is standard and it is not here reported for notational simplicity (the interested reader can refer to Rawlings et al., 2017).

3. Thermal load forecasting

As mentioned in Section 2.2, the DHNet thermal demand could be not measured in real-time at the Novate Milanese plant. Moreover, its forecasts are necessary for the day-ahead optimization phase, where the DHS must plan its optimal operation for the next day. Thanks to the availability of many historical weather and load data measured at the plant, a load forecasting algorithm could be effectively trained. Precisely, the developed load forecasting system is designed to predict the total DHNet thermal demand profile for the whole day d, denoted as $\{\hat{P}_{u,tot}^{th,d}(1), \dots \hat{P}_{u,tot}^{th,d}(N)\}$, using data available at the day $d-1$.

As reported in Bianchi, Castellini, Tarocco, and Farinelli (2019), many possible inputs, or features, can be used for the thermal load forecasting algorithm, such as the thermal demand at previous days or the forecasted solar radiation, wind, ambient temperature, humidity, etc. To select the best features, load and weather data in 2020 and 2021 has been collected and the correlation between the total DHNet thermal demand and the different features has been then analysed. Eventually, the three input variables with highest correlation with the thermal demand on day d have been selected: (i) the thermal load profile at day $d-1$, and (ii) the forecasted solar radiation and (iii) the forecasted ambient temperature for day d, available on the previous day.

For the considered problem, different machine learning techniques can be applied, as discussed in Zdravković, Ćirić, and Ignjatović (2022). Among the available methods, the Support Vector Regression (SVR) method has been implemented given its tuning simplicity and the obtained satisfactory performances. More details on the adopted machine learning approach are discussed in Al-Shammari et al. (2016). Precisely, a multi-output SVR model is designed, where M different prediction models are constructed to predict the M future values of the output variable based on the past input data (Bao, Xiong, & Hu, 2014). Thus, the total thermal demand $\forall t \in \mathcal{T} = \{1, \dots, M\}$ of the next day d is estimated as

$$\hat{P}_{u,tot}^{th,d}(t) = \hat{\Phi}_t \left(P_{u,tot}^{t,d-1}(1, \dots, M), \, \hat{R}^d(1, \dots, M), \, \hat{T}_{amb}^d(1, \dots, M) \right) \tag{28}$$

where $P_{u,tot}^{t,d-1}$ represents the total thermal demand at the previous day $d-1$, while $\hat{R}^d$ and $\hat{T}_{amb}^d$ are the forecasted profiles of the solar radiation and ambient temperature for day d, respectively. It is worth noting that other features could be included, such as the current day of the week or the month. These have been not taken into account since satisfying performances are achieved using the selected features,

i.e., the ones with the highest correlation with the output, considering as test different random days over the year, both during week and the weekend. The performances of the designed forecasting algorithm are reported in Section 5.

4. Day-ahead optimization and online MPC formulation

Once the overall DHS model is defined, the optimization and control problem can be formulated. This will regulate thermal generators operations maximizing the DHS efficiency and profit from the participation to the day-ahead energy market. To accomplish these tasks, the DHS system must be optimized in two phases:

- *Day-ahead optimization*: This serves to schedule the optimal power profile exchanged by the DHS plant with the electrical grid for the next day. This is computed considering selling and buying energy prices, defined by the Day-Ahead Energy Market, the available load forecasts and local production costs, meanwhile ensuring the satisfaction of all network constraints (La Bella, Farina, Sandroni, & Scattolini, 2019). The obtained day-ahead power profile must be then communicated to electrical system operators.
- *Online control*: The communicated electrical power profile must be tracked during the day despite unforeseen load or production changes (Bonassi, La Bella, Lazzari, Sandroni, & Scattolini, 2021). System operators could also request to vary the electrical power profile for specific time-slots based on the needs of the electrical system, requesting the so-called balancing services (La Bella, Falsone, Ioli, Prandini, & Scattolini, 2021). Therefore, the DHS plant must be controlled during the online operation to track the imposed electric power references.[1] On the other hand, the thermal load demand may easily vary with respect to forecasts changing the thermal conditions of the DHNet and so the required thermal power to the heating station. Therefore, the online control is required to operate in closed-loop, exploiting actual measurements from plant to continuously optimize the overall DHS. For this task, an MPC regulation strategy is proposed (Rawlings et al., 2017).

4.1. Day-ahead optimization problem

The day-ahead optimization problem is solved offline (one day before) considering the 24 h of operation of the DHS plant of the next day. Introducing the vector of the main optimization variables

$$\sigma = \Big[\left(P^e_{c,i},\, P^{th}_{c,i},\, q^g_{c,i},\, \delta_{c,i} \right)_{\forall i \in \mathcal{N}_c},\, \left(P^e_{b,j},\, P^{th}_{b,j},\, q^g_{b,j},\, \delta_{b,j} \right)_{\forall j \in \mathcal{N}_b},\; P^{e,in}_{hs},\, P^{e,out}_{hs},\, q^w,\, T^s,\, T^r,\, T^u_{\forall j \in \widetilde{L}} \Big],$$

the day-ahead problem is formulated as

$$\min_{\sigma(1),\dots,\sigma(M)} \sum_{\forall t \in \mathcal{T}} \Big(\pi^{e,b}(t)\,\tau\, P^{e,in}_{hs}(t) - \pi^{e,s}(t)\,\tau\, P^{e,out}_{hs}(t) + \pi^g(t)\,\tau\, c^g_{lhv} \Big(\sum_{i=1}^{n_c} q^g_{c,i}(t) + \sum_{j=1}^{n_b} q^g_{b,j}(t) \Big) \Big) \tag{29a}$$

subject to, $\forall\, t \in \mathcal{T}$,

$$\left.\begin{array}{ll} (1)\text{–}(3), & \forall i \in \mathcal{N}_c, \quad \text{(cogenerators)} \\ (8)\text{–}(10), & \forall j \in \mathcal{N}_b, \quad \text{(boilers)} \\ (22),\ (25), & \forall j \in \widetilde{L}, \quad \text{(users)} \\ (6),\ (12),\ (13),\ (16),\ (17), & \quad \text{(heating station)} \\ (20),\ (23),\ (24),\ (26),\ (27), & \quad \text{(DHNet)} \end{array}\right\} \tag{29b}$$

[1] The participation to intra-day energy markets is not here considered but this could be included in the online control phase, redefining the electrical power profile based on the current energy prices.

As evident from (29a), the objective of the day-ahead problem is to maximize electrical energy trading profit, considering buying and selling energy prices, i.e., $\pi^{e,b}$ and $\pi^{e,s}$, respectively, and to minimize the cost for the local gas consumption, considering the gas price π^g. Thanks to the adopted modelling methodology, and to the considerations in Remark 2.1, (29) can be formulated as a Mixed-Integer Linear Problem (MILP), which can be easily optimized by common solvers (e.g. CPLEX, GUROBI etc.). In fact, constraints (6), (12), (17), (22) and (23) can be reformulated as linear mixed-integer ones using methods described in Bemporad and Morari (1999).

It is worth noting that the identified DHNet temperature models (22) and (23) depend on past inputs and outputs, and their values are set equal to the corresponding DHS plant measurements available on the day-ahead.

4.2. Model predictive control design

An MPC regulation system is designed to periodically optimize the DHS plant during the daily operation. This is executed at each time instant $t \in \mathcal{T}$ and it considers a prediction horizon $\mathcal{T}_t = \{t, \dots, M\}$ of $N(t) = M - t + 1$ steps, according to the *shrinking horizon* principle (Rawlings et al., 2017). In the following, the index k is used to span over the prediction horizon, i.e., $k \in \mathcal{T}_t = \{t, \dots, M\}$. The shrinking predictive control strategy is used as it enables to consider at each sampling time t a prediction horizon $\mathcal{T}_t = \{t, \dots, M\}$ which spans from the current time instant, i.e., $k = t$, until the end of the day, i.e., $k = M$, that are the time instants where the day-ahead solution provided by (29) is available.

As mentioned, the online control problem serves to track, or to properly vary upon external requests, the DHS electrical power profile computed by the day-ahead problem (29), here indicated as $P^{e,*}_{hs}$. Thus, the following constraint is stated

$$P^e_{hs}(k) = P^{e,*}_{hs}(k) + \Delta \widetilde{P}^e_{hs}(k) + \epsilon^e(k), \tag{30}$$

where $k \in \mathcal{T}_t$, the parameter $\Delta \widetilde{P}^e_{hs}$ expresses possible variations on the day-ahead electrical power profile requested by system operators, while ϵ^e is a slack variable accounting for power imbalances, strongly minimized to avoid penalties. Thus, the MPC cost function to be minimized at each $t \in \mathcal{T}$ is

$$J(t) = \sum_{\forall k \in \mathcal{T}_t} \Big(\pi^{e,i}(k)\,\tau\,|\epsilon^e(k)| + \pi^g(k)\,\tau\, c^g_{lhv} \Big(\sum_{i=1}^{n_c} q^g_{c,i}(k) + \sum_{j=1}^{n_b} q^g_{b,j}(k) \Big) \Big), \tag{31}$$

where the control objective is to minimize electrical power mismatches, through the imbalance cost $\pi^{e,i}$, and the cost for the local gas consumption. The cost function (31) is not linear due to the presence of the absolute value on the first term. In order to keep also the online problem in MILP form, the epigraphic reformulation is adopted. In particular, introducing an auxiliary variable h^e and the following constraint

$$h^e(k) \geq \epsilon^e(k), \quad h^e(k) \geq -\epsilon^e(k), \tag{32}$$

the cost function (31) can be rewritten as

$$J^h(t) = \sum_{\forall k \in \mathcal{T}_t} \Big(\pi^{e,i}(k)\,\tau\, h^e(k) + \pi^g(k)\,\tau\, c^g_{lhv} \Big(\sum_{i=1}^{n_c} q^g_{c,i}(k) + \sum_{j=1}^{n_b} q^g_{b,j}(k) \Big) \Big),$$

which now is linear.

For the sake of completeness, it is explicitly stated that the closed-loop MPC regulator initializes the DHNet models (22) and (23) at each $t \in \mathcal{T}$ using the real measurements from the DHS plant. Introducing the vector $z = [T^s, T^r, T^u_{\forall j \in \widetilde{L}}]$, it holds that

$$z(t-i) = \tilde{z}(t-i), \qquad \forall i \in \{0, \dots, \bar{n}\}, \tag{33}$$

where $\tilde{z}$ indicates the measured variables and $\bar{n}$ the maximum order of the identified models (22) and (23). Thermal demand measurements,

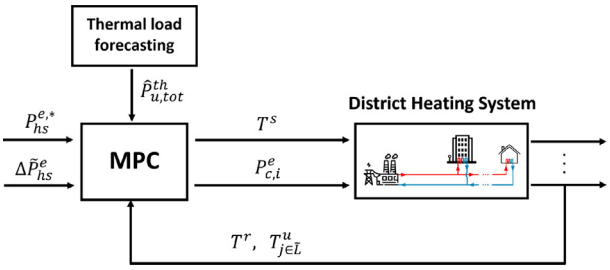

Fig. 3. Schematic of the control diagram for the online MPC regulation of DHSs.

also necessary in (22) and (23), were not available in real-time at the DHS Novate Milanese plant and therefore the forecasted values (28) have been still used during the experiments. As it will be evident in Section 5, exploiting closed-loop measurements significantly improve the prediction performances of the identified DHNet models with respect to the open-loop case.

Therefore, the shirking-horizon MPC problem, solved at each $t \in \mathcal{T}$, is

$$\min_{\sigma(t),\dots,\sigma(M)} \quad J^h(t)$$

subject to, $\forall k \in \{t,\dots,M\}$,

(29b), (DHS constraints), (34)

(30), (32), (Electrical power reference),

(33), (DHNet models initialization),

which, also in this case, is a MILP.

For the sake of clarity, the control diagram of the designed online MPC regulator is reported in Fig. 3, specifying the control inputs (DHNet supply temperature and cogenerators power), the measured variables (DHNet return temperature and supply temperature at critical users), the forecasted disturbance (total thermal demand) and the reference (day-ahead scheduled electrical profile and eventual variations requested by system operators).

5. Case study

The proposed optimization and control strategy has been tested on the Novate Milanese DHS plant. This is constituted of a central heating station with $n_c = 2$ cogenerators and $n_b = 4$ gas boilers, and a radial DHNet. The characteristics of the devices at the central heating station are reported in Table 2. The DHNet, depicted in Fig. 4, has an extension of around 5 km, with 480 m^3 of flowing water and 45 connected users' substations (83% residential, 10% public and 7% commercial).

The designed control system has been tested firstly in simulation, using a DHS simulator developed in TRNSYS®, and successively with experiments on the real plant. The simulation environment has been developed using the real characteristics of the network, such as pipes diameters, lengths and heat transfer coefficients, which have been provided by the energy company A2A. As common in the simulation of large-scale networks, the simulation environment have been developed by grouping few close users into equivalent districts. In particular, an approach similar to Larsen, Bøhm, and Wigbels (2004) has been adopted, where the corresponding pipes in each district are aggregated by maintaining the same equivalent volume and surface of heat exchange. Given the imposed DHNet supply temperature, the water flow and the thermal demand of each user, the developed simulator returns as output the dynamical response of the water temperature at each point of the DHNet, considering heat transport delays and thermal losses. The developed simulator has been extensively validated with the real plant data, achieving an average Mean Absolute Percentage Error (MAPE) of 0.7%. Fig. 5 reports the dynamical response of DHNet return temperature in a simulation of one week, precisely between March 8th and March 14th, 2021, comparing the result with the real measurement from the plant.

Despite the high simulation performances, the results of the proposed control strategy with respect to the real plant experiments will reported in the following, being them more significant for assessing the real achievable performances. Firstly, the validation of the proposed data-based DHNet models and of the thermal load forecasting with respect to real data is discussed. Then, the control experiments and performances for different test days are presented.

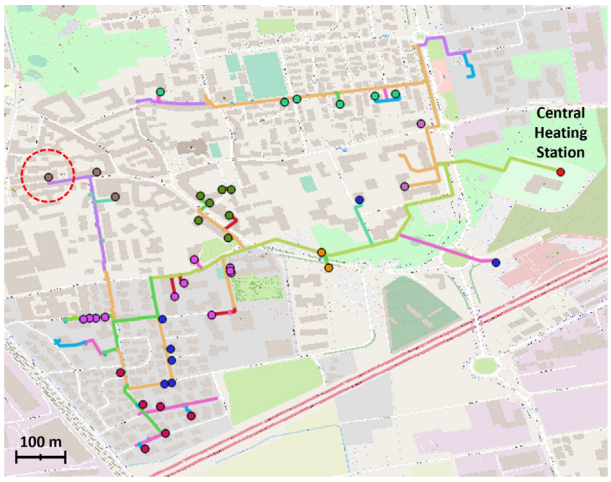

Fig. 4. Geographic Information System (GIS) map of the Novate Milanese district heating network. On the right, the central heating station is located, which coordinates are 45.53183 North, 9.14908 East. The red dashed circle indicates the position of the selected user for the supply temperature identification, which coordinates are 45,53172 North, 9.13822 East.

Table 2
Parameters for the central heating station of the Novate Milanese plant.

Cogenerators, $n_c = 2$		
$\left(\overline{P}^e_{c,i}, \underline{P}^e_{c,i}\right)_{i=1,\dots,n_c}$	(526, 260)	kW
$\left(\eta^{th}_{c,i}, \eta^e_{c,i}\right)_{i=1,\dots,n_c}$	(0.45, 0.38)	
$\left(\tilde{P}^{e,aux}_{c,i}\right)_{i=1,\dots,n_c}$	12	kW
$\left(\tilde{q}^w_{c,i}\right)_{i=1,\dots,n_c}$	30	m^3/h
Gas boilers, $n_b = 4$		
$\left(\overline{P}^{th}_{b,j}, \underline{P}^{th}_{b,j}\right)_{j=1,\dots,n_b-1}$	(3300, 200)	kW
$\overline{P}^{th}_{b,n_b}, \underline{P}^{th}_{b,n_b}$	(1300, 200)	kW
$\left(\eta^{th}_{b,j}\right)_{j=1,\dots,n_b}$	0.9	
$\left(\tilde{P}^{e,aux}_{b,j}\right)_{j=1,\dots,n_b}$	17	kW
$\tilde{P}^{th}_b$	3000	kW
Pump system		
H_p	30	m
η_p	0.75	

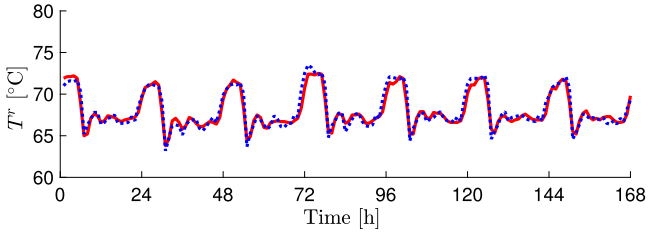

Fig. 5. DHNet return temperature T^r between March 8th and March 14th, 2021: measured data from the plant (solid red) and simulated data (dotted blue).

Table 3
Mean Absolute Percentage Error (MAPE) of the simulator and the identified models with respect to real plant data for the supply temperature at the furthest user.

MAPE	Simulation	Data-based piece-wise model	
T^u	(open-loop)	(open-loop)	(closed-loop)
08.03.2021	0.63%	1.59%	0.79%
09.03.2021	0.89%	1.6%	0.81%
1.12.2021	1.27%	1.91%	0.85%
2.12.2021	1.48%	1.2%	0.81%

Table 4
Mean Absolute Percentage Error (MAPE) of the simulator and the identified models with respect to real plant data for the return DHNet temperature.

MAPE	Simulation	Data-based piece-wise model	
T^r	(open-loop)	(open-loop)	(closed-loop)
08.03.2021	1.36%	1.74%	1.13%
09.03.2021	1.59%	1.46%	1.16%
1.12.2021	1.83%	2.16%	1.43%
2.12.2021	1.71%	1.52%	1.20%

5.1. Data-based model validation

The data-based piece-wise models describing the main DHNet temperatures, i.e., (22)–(23), have been identified using 30 days of training data for each water flow level. In fact, given the impossibility of arbitrary stress the real DHS plant, training data has been generated using the simulator developed in TRNSYS®, applying persistence exciting signals to the supply DHNet temperature and to the thermal demand for each water flow level. Based on the knowledge of real plant data, the following water flow levels have been selected, considering the whole plant operational range and the typical measured flow values at the plant,

$$q^w(t) \in \{100, 125, 150, 175, 200, 225, 250, 300, 350, 400\}\ \mathrm{m}^3/\mathrm{h}\,. \tag{35}$$

Note that the number of water flow levels in (35) has been chosen as a trade-off between modelling accuracy and the complexity of the formulated optimization problem. As previously described, a different ARX model is identified for each water flow level, leading to a piece-wise linear modelling. In particular, two piece-wise ARX models have been identified for the experimental tests: one for the supply temperature at the furthest user from the central heating station along DHNet pipelines, which position is reported in Fig. 4, and one for the DHNet return temperature. The identified piece-wise models have been validated with the real plant data, using the measured DHNet supply temperature and thermal demand as inputs, while the measured DHNet water flow has been approximated, at each time instant, to the closest water flow level in (35).

The model prediction performances with respect to four days are hereafter presented, being these days related to the test experiments that will be described in Section 5.3. Tables 3 and 4 report the MAPE for the identified DHNet temperatures, i.e., the supply temperature at the furthest user and the return DHNet temperature, respectively, with respect to the real plant data.

In particular, the open-loop simulation performances are reported, meaning that 24 h simulations are performed using the measured supply temperature, thermal demand and water flow as inputs. The piece-wise ARX models are tested both in open-loop and in closed-loop, the latter meaning that the measurements of the identified temperatures are used to initialize models at each sampling time. The closed-loop test is reported to resemble the performances of prediction model used by the online MPC regulator, where the system state is measured at each control iteration. As evident from Tables 3 and 4, the identified piece-wise models achieve quite satisfactory performances. Their MAPE prediction error in open-loop is often higher with respect to the simulation one, being the latter a more detailed model, but it remains considerably small, reaching a maximum of 2.16%. On the other hand, if the measured state is fed to the model at each time step, much better performances are achieved, with an average MAPE of 0.8% for the supply temperature to the furthest user, and an average MAPE of 1.2% for the return DHNet temperature. Fig. 6 reports the temperatures predicted by the identified piece-wise ARX models in open-loop and in closed-loop when compared with real plant data on a specific day.

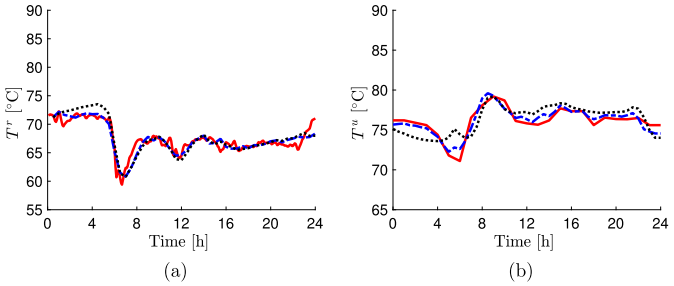

Fig. 6. (a) DHNet return temperature T^r, and (b) supply temperature at the furthest user T^u on March 9th, 2021: closed-loop model prediction (dashed blue), open-loop model prediction (dotted black), real plant data (solid red).

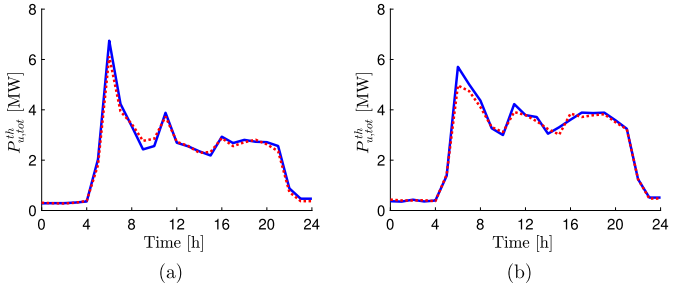

Fig. 7. Forecasting results for the total thermal demand $P^{th}_{u,tot}$ on March 9th (a) and on December 2nd (b), 2021: 24 h forecasted profile (dotted red) and real data (solid blue).

5.2. Thermal load forecasting

As previously discussed, a tool to forecast the DHS thermal demand has been developed. The company A2A S.p.A. provided thermal demand data for the whole 2020/2021 heating season, i.e., between October 2020 to March 2021, while the corresponding solar radiation and environment temperature data period, necessary to predict the thermal demand (see (28)), have been measured and provided by ARPA Lombardia, i.e., an Italian regional agency for the environment protection (ARPA Lombardia, 0000). The whole dataset has been divided in training and validation data, the latter comprising a random day for each month in the 2020/2021 heating season. The SVR forecasting model in (28) has been trained using the *scikit–learn* Python library, setting the *radial-basis function* as kernel (Pedregosa et al., 2011). Considering the validation set, the identified SVR forecasting model achieves an average MAPE of 7.3%. Fig. 7 reports the forecasted and the real thermal demand for two test days.

5.3. Experimental results

The Novate Milanese DHS plant is managed and monitored through a control room located in the central heating station. The proposed optimization and control strategy has been implemented on a personal laptop using the software environment IBM ILOG CPLEX Optimization Studio®, writing/reading proper files with measurements and control

inputs at the plant control room. The overall system has been tested for few days, compatibly with the availability of A2A S.p.A., considering that the Novate DHS plant is always on service (also during summer for the hot domestic water delivery).

The considered plant is normally regulated by a rule-based control logic defined by A2A S.p.A.. This can be synthesized in the following points: (i) the reference for the output temperature of gas boilers is fixed for the whole day, and it is monthly varied by A2A plant operators based on the expected thermal demand; (ii) gas boilers are deactivated during the night, i.e., between 22:00 and 5:00, while during the day are operated according to the local internal logic (described in Section 2.1.1); (iii) among the two cogenerators, one is always active at maximum power, while the other is always kept off. This last choice is considered a good compromise, since selling electrical energy to the grid implies an economical gain but cogenerators are less efficient then gas boilers for thermal energy production.

In the following, the test days where the proposed optimization and control strategy is applied are compared with other days where a similar thermal demand was recorded and the local rule-based logic was operating the plant. For a proper comparison between the performances of two strategies, specific Key Performance Indexes (KPI) are analysed. These are:

- *Produced electrical energy*, i.e.,

$$E^{el}_{\text{DHS}} = \sum_{t=1}^{M} \tau \, P^{e}_{hs}(t).$$

- *Consumed gas volume*, i.e.,

$$Q^{g}_{\text{DHS}} = \sum_{t=1}^{M} \tau \left(\sum_{i=1}^{n_c} q^{g}_{c,i}(t) + \sum_{j=1}^{n_b} q^{g}_{b,j}(t) \right).$$

- *Operational cost*, i.e.

$$J_{\text{DHS}} = \sum_{t=1}^{M} \Bigg(\pi^{e,b}(t) \, \tau \, P^{e,in}_{hs}(t) - \pi^{e,s}(t) \, \tau \, P^{e,out}_{hs}(t) + \\ + \pi^{g}(t) \, \tau \, c^{g}_{lhv} \left(\sum_{i=1}^{n_c} q^{g}_{c,i}(t) + \sum_{j=1}^{n_b} q^{g}_{b,j}(t) \right) \Bigg).$$

- *Primary Energy Factor* (PEF), that is a standardized index to assess DHS efficiency (Noussan, 2018). This is the ratio between the DHS consumed primary energy, discounted by the produced electrical energy, and the one delivered to final users. Precisely, the PEF is defined as

$$\text{PEF}_{\text{DHS}} = \frac{f_g \, Q^{g}_{\text{DHS}} \, c^{g}_{lhv} - f_e \, E^{el}_{\text{DHS}}}{\sum_{t=1}^{M} \tau \, P^{th}_{u,tot}(t)}, \tag{36}$$

  where the weights f_g and f_e are the PEF of the single energy sources, i.e., the gas fuel and the electricity, in this case. These weights take into account also other factors (e.g., transportation costs) and they are set as $f_g = 1.04$ and $f_e = 2.42$ in the following, representing the Italian scenario (Latõšov, Volkova, Siirde, Kurnitski, & Thalfeldt, 2017).
- *Effective gas consumption*, considering the whole energy system. In fact, the higher is the electrical energy produced by the DHS cogenerators, the lower is the energy that the overall electrical system has to produce to satisfy the electricity demand. Therefore, the following index is introduced

$$Q^{g}_{\text{eff}} = Q^{g}_{\text{DHS}} - c^{g}_{lhv} \frac{E^{el}_{\text{DHS}}}{\eta_{es}},$$

  where the gas consumed by the DHS is discounted by the gas saved by the electrical system for not producing E^{el}_{DHS}, with η_{es} representing the conversion efficiency. Here, $\eta_{es} = 0.55$ is considered, being the efficiency of a typical combined-cycle power plant, a system that can potentially reduce its production in the face of the DHS cogenerators one.
- *Effective CO_2 emission*, considering the effective gas consumption related to the whole energy system. This is defined as

$$G^{e}_{\text{eff}} = Q^{g}_{\text{eff}} \, c^{g}_{lhv} \, e_g,$$

  where $e_g = 0.2 \, \frac{kg}{kWh}$ is the CO_2 emission factor of natural gas (Latõšov et al., 2017).

In the following, two test days are reported where the proposed control strategy was applied, i.e, March 9th and December 2nd, 2021. The two test days are different not only with respect to the thermal demand, generally higher in December, but also because it was not possible to arbitrary control cogenerators in March 2021 due to technical reasons. Although being a limitation for the energy market participation, this gives the opportunity to analyse the cost minimization achieved just with respect to the gas consumption reduction. The additional gain derived from the participation to the day-ahead energy market is evident in the tests on December 2nd, where cogenerators were optimally managed.

The electrical energy and gas prices used for tests were given by the day-ahead Italian Energy Market, and they are available in the online database (GME, 0000). For both test days, the identified DHNet temperatures are bounded as follows. The lower bound of the supply temperature at the selected user (i.e. the furthest one) is set as $\underline{T}^{u}(t)$ =75 °C between 7:00 and 21:00, and $\underline{T}^{u}(t)$ =70 °C during the night. The upper and lower bounds of the DHNet return temperature are imposed as $\overline{T}^{r}(t) = 67$ °C and $\underline{T}^{r}(t) = 63$ °C between 7:00 and 21:00, and as $\overline{T}^{r}(t) = 75$ °C and $\underline{T}^{r}(t) = 55$ °C during the night.

5.3.1. Experiments in March without cogeneration control

The control experiments performed on March 9th, 2021 are compared with another day where the standard rule-based logic was applied and a similar thermal demand was measured, that is March 8th, 2021. The thermal demand profiles of the two days are shown in Fig. 8(c). For both days, it was not possible to optimize cogenerators for technical reasons. Thus, one cogenerator was constantly operated at maximum power, the other was kept off, and only gas boilers' outlet temperature could be operated by the proposed control strategy. The DHnet supply water temperature measured on the two days is illustrated in Fig. 8(a), together with the imposed lower and upper bound, i.e., $\underline{T}^{s} = 70$ °C and $\overline{T}^{s} = 83$ °C. According to the rule-based logic, the outlet temperature of gas boilers is normally fixed at 83 °C in March. Therefore, the DHNet supply temperature was maintained at that value between 5:00 and 22:00 on March 8th, while it decreased during the night as boilers were turned off and just one cogenerator was active (see dotted red line in Fig. 8(a)). On the other hand, the developed MPC control system, applied on March 9th, continuously varied the outlet temperature of gas boilers, so as to increase it in correspondence of the thermal load peaks. This modulation has a direct impact on the supply temperature of users. Fig. 8(e) reports the measured supply temperature at the furthest user on March 8th and 9th, showing a lower temperature profile on the day when the MPC control was applied, but always respecting the imposed lower bound. The supply temperatures measured at different users on March 9th are depicted in Fig. 8(f), showing that imposing the lower bound to few critical points (e.g., the to the furthest user) enables the satisfaction of lower bound for the whole DHNet. Fig. 8(b) depicts the measured DHNet return temperature, showing also in this case a slightly lower temperature profile for the day when the MPC control was applied. Finally, the DHNet water flow is shown in 8(d), higher when the supply temperature was decreased by the MPC control system, so as to properly satisfy the thermal demand.

The achieved KPI by the rule-based operation and by the MPC regulation on March 8th and 9th, respectively, are reported in Table 5. For the sake of completeness, also the average performances achieved on few days around tests are reported. In particular, the supplied electrical energy did non vary, as cogenerators could not be differently

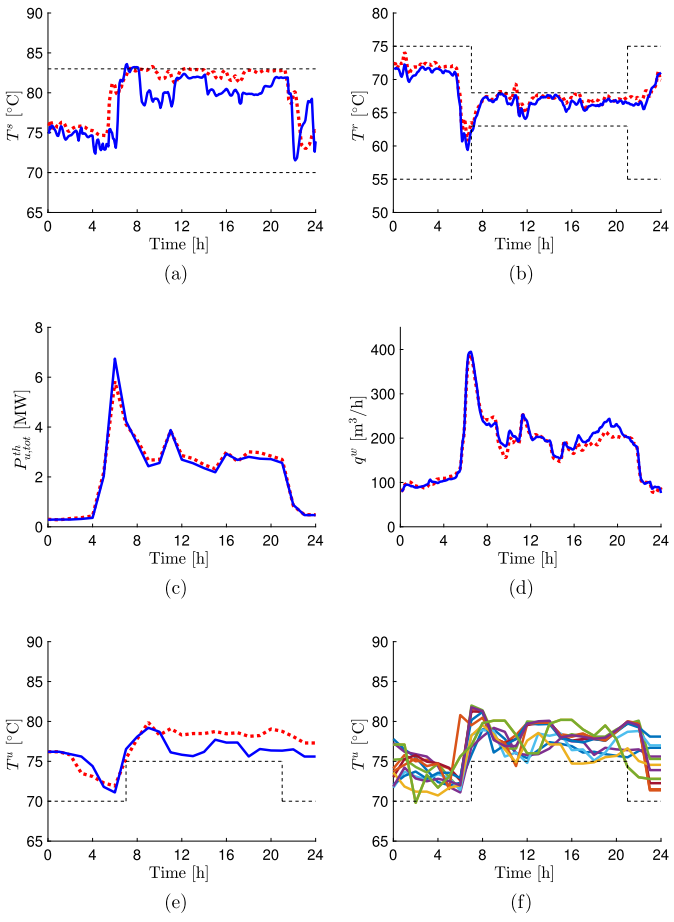

Fig. 8. Measured plant data on March 8th, 2021 (rule-based logic, dotted red) and on March 9th, 2021 (MPC strategy, solid blue): (a) DHNet supply temperature T^s, (b) DHNet return temperature T^r, (c) users total thermal demand $P^{th}_{u,tot}$, (d) DHNet water flow q^w, (e) supply temperature at the identified user T^u, (f) measured supply temperatures at different users on March 9th, 2021 (MPC strategy).

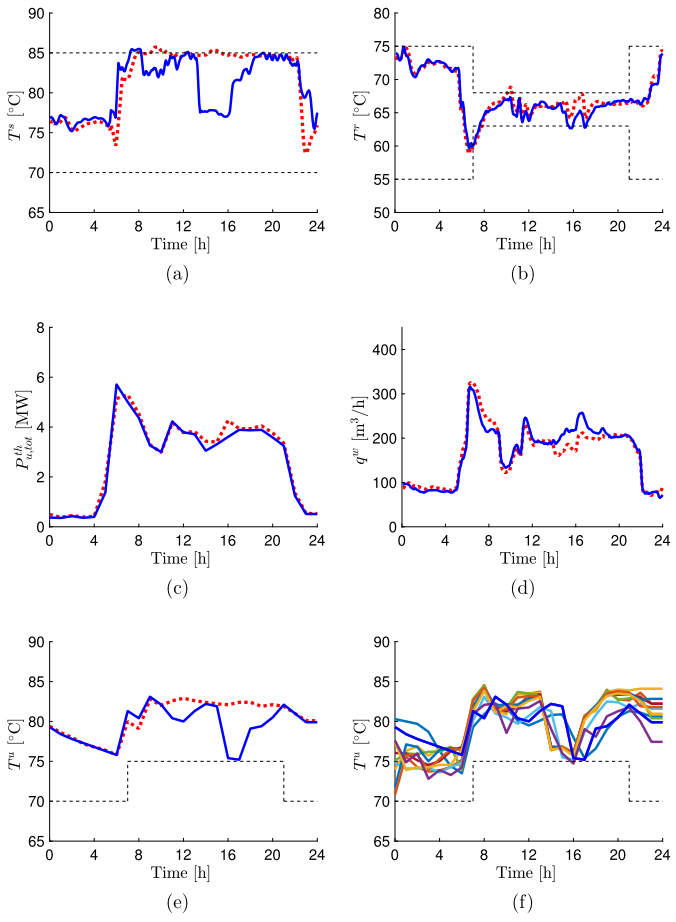

Fig. 9. Measured plant data on December 1st, 2021 (rule-based logic, dotted red) and on December 2nd, 2021 (MPC strategy, solid blue): (a) DHNet supply temperature T^s, (b) DHNet return temperature T^r, (c) users total thermal demand $P^{th}_{u,tot}$, (d) DHNet water flow q^w, (e) supply temperature at the identified user T^u, (f) measured supply temperatures at different users on December 2nd, 2021 (MPC strategy).

Table 5
Key Performance Indexes achieved by the proposed control strategy in comparison to the rule-based operation for the tests in March 2021. The percentage values are computed comparing March 8th and 9th, 2021.

KPI	Rule-based operation		MPC control	
	6.03–11.03.21 (average)	8.03.21	9.03.21	
E^{el}_{DHS} [MWh]	11.5	11.5	11.5	(+0%)
Q^g_{DHS} [Smc]	7645	7790	7430	(−4.6%)
J_{DHS} [€]	618	645	582	(−9.7%)
PEF_{DHS}	0.95	0.96	0.91	(−5.2%)
Q^g_{eff} [Smc]	5532	5682	5323	(−6.3%)
G^e_{eff} [tCO2]	11	11.29	10.58	(−6.3%)

modulated during the tests. On the other hand, the MPC regulation enabled to save a significant amount of consumed gas (i.e., 360 Smc) through the optimal modulation of the DHNet supply temperature, which directly resulted in lower operational costs. Considering the PEF index, this also decreased when the MPC regulation was applied, implying that less primary energy was consumed for satisfying the thermal demand (see (36)). Finally, the effective consumed gas and CO_2 emissions considering the whole energy system showed also a consistent reduction, despite cogenerator production could not be optimized.

5.3.2. Experiments in december with cogeneration control

The designed optimization and control strategy was tested on December 2nd, 2021, with the participation to the day ahead energy market. Also in this case, a similar day is considered to properly compare the obtained performances, i.e., December 1st, 2021. The thermal demand profiles of the two days are reported in Fig. 9(c).

Given the high convenience of selling electrical energy to the grid, the solution of the day-ahead optimization problem for December 2nd consisted in maintaining a cogenerator at maximum power for the whole day, while the other is operated at maximum power between 5:00 and 23:00, and kept off during the night given the low thermal demand. The implemented MPC control system operated the overall DHS to track the pre-defined electrical power profile, as reported in Fig. 10(a), coordinating cogenerators electrical production as pre-scheduled, as shown in Fig. 10(b).

Fig. 9(a) reports the DHNet supply temperature profile for the two considered days, together with the imposed lower and upper bound, i.e., $\underline{T}^s = 70$ °C and $\overline{T}^s = 85$ °C. According to the rule-based logic, the outlet temperature of gas boilers is normally set to 85 °C in December. As evident, also in this case the MPC action consisted in frequent variations of the DHNet supply temperature, without violating the lower bound of the furthest user supply temperature, as illustrated in Fig. 9(e). The supply temperatures at different users of the DHNet are depicted in Fig. 9(f), still respecting the requested lower bound. Also in this case, the DHNet return temperature is lower when the proposed control strategy was applied, but it is still maintained within the imposed operational range. Finally, Fig. 9(d) shows the DHNet water flow, generally higher when the DHNet supply temperature is decreased so as to satisfy the thermal demand.

The recorded KPI for the test days are reported in Table 6, together with the average values for few days around the tests. The proposed

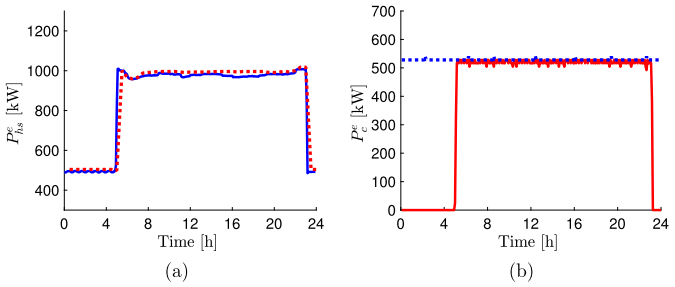

Fig. 10. (a) Day-ahead (dashed red) and real measured (solid blue) DHS electrical power profile P^e_{hs} for December 2nd, 2021. (b) Electrical power production P^e_c of cogenerator 1 (dashed blue) and cogenerator 2 (solid red) measured on December 2nd, 2021.

Table 6
Key Performance Indexes achieved by the proposed control strategy in comparison to the rule-based operation for the tests in December 2021. The percentage values are computed comparing December 1st and 2nd, 2021.

KPI	Rule-based operation		MPC Control	
	29.11–04.12.21 (average)	1.12.21	2.12.21	
E^{el}_{DHS} [MWh]	11.44	11.41	20.9	(+83%)
Q^g_{DHS} [Smc]	9098	9200	10290	(+11.8%)
J_{DHS} [€]	5780	5891	4233	(−26.8%)
PEF_{DHS}	0.99	0.99	0.85	(−14.4%)
Q^g_{eff} [Smc]	7006	7114	6466	(−9.1%)
G^e_{eff} [tCO2]	13.93	14.15	12.85	(−9.1%)

optimization and control strategy has a direct impact on the produced electrical energy, which is doubled, but it also implied a higher gas consumption. This is due to the lower thermal efficiency of cogenerators with respect to gas boilers.

On the other hand, the optimal use of cogenerators results in a consistent reduction of operational costs with respect to the standard operation, as more electrical energy is sold to the energy markets.[2]

Considering the PEF index, it is evident that a significant reduction is achieved, since the benefits given by the additional produced electrical energy overcome the increase of primary energy consumption due to cogenerators operation. This is also highlighted by the effective consumed gas and CO_2 emissions considering the overall energy system, recording significant reductions when the MPC strategy is applied.

5.4. Computational performance

The described experimental tests have been performed using a personal laptop located in the plant control room, with an Intel i7-11850H processor, and solving the optimization and control problems with the software environment IBM ILOG CPLEX Optimization Studio®. Considering the computational performances, the day-ahead optimization problem (29) has been solved with an average computing time of 2 min and 19 s (it is recalled that this problem is solved offline). The online MPC control problem is characterized by a computational time depending on the prediction horizon length, which varies over the day due to the adopted shrinking horizon approach. In particular, it has been derived from the experimental tests that the average computational time for solving (34) is $39.2 + 0.46\,N(t)$ seconds, where $N(t) = (M - t + 1)$ is the prediction horizon length at the generic time instant $t \in \mathcal{T}$. In particular, the maximum average computational time is 61.3 s, largely lower than the control sampling time.

[2] Note that the recorded costs are much higher with respect to the ones in March due to the energy crisis affecting that period, implying higher energy and gas prices.

6. Conclusions

This paper addressed the design of an optimization and predictive control strategy for district heating systems, enabling the reduction of energy consumption to satisfy the thermal demand and the cost-effective participation to day-ahead electricity markets. The designed system exploits a combination of mathematical and identified data-based models, able to accurately represent the DHS system. The developed control system has been tested for few days on a real plant, owned by the energy company A2A S.p.A. and located in Novate Milanese (Italy). The measured control performances are compared with the ones of the standard rule-based operation, showing that operational costs and the effective gas consumption are significantly reduced when the designed control system is applied.

Future developments regard the design of learning-based predictive control systems, exploiting online measured data to improve accuracy of the identified models, e.g., using techniques proposed in Breschi et al. (2016), with tests on real plant case-studies. Moreover, the investigation of multi-objective optimization strategies can be of interest, defining a methodology to optimally coordinate different objectives in DHSs, such as the electricity market participation and the thermal efficiency maximization.

Declaration of competing interest

The authors declare that they have no known competing financial interests or personal relationships that could have appeared to influence the work reported in this paper.

Acknowledgement

The authors want to thank A2A S.p.A. for the fruitful research collaboration and, in particular, Eng. Andrea Scaburri for its valuable support during the tests.

The research activity has been financed by the Research Fund for the Italian Electrical System under the Contract Agreement between RSE S.p.A. and the Ministry of Economic Development - General Directorate for the Electricity Market, Renewable Energy and Energy Efficiency, Nuclear Energy in compliance with the Decree of April 16th, 2018.

References

Al-Shammari, E. T., Keivani, A., Shamshirband, S., Mostafaeipour, A., Yee, L., Petković, D., et al. (2016). Prediction of heat load in district heating systems by support vector machine with firefly searching algorithm. *Energy*, *95*, 266–273.

ARPA Lombardia (0000). Agenzia Regionale per la Protezione dell'Ambiente, https://www.arpalombardia.it/.

Bao, Y., Xiong, T., & Hu, Z. (2014). Multi-step-ahead time series prediction using multiple-output support vector regression. *Neurocomputing*, *129*, 482–493.

Bemporad, A., & Morari, M. (1999). Control of systems integrating logic, dynamics, and constraints. *Automatica*, *35*(3), 407–427.

Benonysson, A., Bøhm, B., & Ravn, H. F. (1995). Operational optimization in a district heating system. *Energy Conversion and Management*, *36*(5), 297–314.

Bianchi, F., Castellini, A., Tarocco, P., & Farinelli, A. (2019). Load forecasting in district heating networks: Model comparison on a real-world case study. In *International conference on machine learning, optimization, and data science* (pp. 553–565). Springer.

Bonassi, F., La Bella, A., Lazzari, R., Sandroni, C., & Scattolini, R. (2021). Supervised control of hybrid AC–DC grids for power balance restoration. *Electric Power Systems Research*, *196*, Article 107107.

Breschi, V., Piga, D., & Bemporad, A. (2016). Piecewise affine regression via recursive multiple least squares and multicategory discrimination. *Automatica*, *73*, 155–162.

Buffa, S., Fouladfar, M. H., Franchini, G., Lozano Gabarre, I., & Andrés Chicote, M. (2021). Advanced control and fault detection strategies for district heating and cooling systems—A review. *Applied Sciences*, *11*(1), 455.

Cengel, Y. A. (2002). *Heat transfer: A practical approach* (2nd ed.). McGraw-Hill.

European Commission (2016). Communication from the commission to the European parliament, the council, the European economic and social committee and the committee of the regions — An EU strategy on heating and cooling. https://eur-lex.europa.eu/legal-content/EN/TXT/?uri=CELEX%3A52016DC0051.

Farahani, S. S., Lukszo, Z., Keviczky, T., De Schutter, B., & Murray, R. M. (2016). Robust model predictive control for an uncertain smart thermal grid. In *2016 European control conference* (pp. 1195–1200). IEEE.

GME (0000). Gestore Mercati Energetici, https://www.mercatoelettrico.org/it/mercati/mercatoelettrico/mpe.aspx.

Golmohamadi, H., Larsen, K. G., Jensen, P. G., & Hasrat, I. R. (2022). Integration of flexibility potentials of district heating systems into electricity markets: A review. *Renewable and Sustainable Energy Reviews*, *159*, Article 112200.

Hewing, L., Wabersich, K. P., Menner, M., & Zeilinger, M. N. (2020). Learning-based model predictive control: Toward safe learning in control. *Annual Review of Control, Robotics, and Autonomous Systems*, *3*, 269–296.

Krug, R., Mehrmann, V., & Schmidt, M. (2021). Nonlinear optimization of district heating networks. *Optimization and Engineering*, *22*(2), 783–819.

La Bella, A., Del Corno, A., & Scaburri, A. (2021). Data-driven modelling and optimal management of district heating networks. In *2021 AEIT international annual conference* (pp. 1–6). IEEE.

La Bella, A., Falsone, A., Ioli, D., Prandini, M., & Scattolini, R. (2021). A mixed-integer distributed approach to prosumers aggregation for providing balancing services. *International Journal of Electrical Power & Energy Systems*, *133*, Article 107228.

La Bella, A., Farina, M., Sandroni, C., & Scattolini, R. (2019). Design of aggregators for the day-ahead management of microgrids providing active and reactive power services. *IEEE Transactions on Control Systems Technology*, *28*(6), 2616–2624.

Lake, A., Rezaie, B., & Beyerlein, S. (2017). Review of district heating and cooling systems for a sustainable future. *Renewable and Sustainable Energy Reviews*, *67*, 417–425.

Larsen, H. V., Bøhm, B., & Wigbels, M. (2004). A comparison of aggregated models for simulation and operational optimisation of district heating networks. *Energy Conversion and Management*, *45*(7–8), 1119–1139.

Latõšov, E., Volkova, A., Siirde, A., Kurnitski, J., & Thalfeldt, M. (2017). Primary energy factor for district heating networks in European Union member states. *Energy Procedia*, *116*, 69–77.

Ljung, L., & Glad, T. (1994). *Modeling of dynamic systems*. USA: Prentice-Hall, Inc..

Lu, M., Zhang, C., Zhang, D., Wang, R., Zhou, Z., Zhan, C., et al. (2021). Operational optimization of district heating system based on an integrated model in TRNSYS. *Energy and Buildings*, *230*, Article 110538.

Machado, J. E., Cucuzzella, M., & Scherpen, J. M. A. (2022). Modeling and passivity properties of multi-producer district heating systems. *Automatica*, *142*, Article 110397.

Machado, J. E., Ferguson, J., Cucuzzella, M., & Scherpen, J. M. A. (2023). Decentralized temperature and storage volume control in multiproducer district heating. *IEEE Control Systems Letters*, *7*, 413–418.

Noussan, M. (2018). Performance indicators of district heating systems in Italy–Insights from a data analysis. *Applied Thermal Engineering*, *134*, 194–202.

Paardekooper, S., Lund, R. S., Mathiesen, B. V., Chang, M., Petersen, U. R., Grundahl, L., et al. (2018). *Heat roadmap Europe 4: Quantifying the impact of low-carbon heating and cooling roadmaps*. Aalborg Universitetsforlag, https://vbn.aau.dk/en/publications/heat-roadmap-europe-4-quantifying-the-impact-of-low-carbon-heatin.

Pedregosa, F., Varoquaux, G., Gramfort, A., Michel, V., Thirion, B., Grisel, O., et al. (2011). Scikit–learn: Machine learning in Python. *Journal of Machine Learning Research*, *12*, 2825–2830.

Quaggiotto, D., Vivian, J., & Zarrella, A. (2021). Management of a district heating network using model predictive control with and without thermal storage. *Optimization and Engineering*, *22*(3), 1897–1919.

Rathod, N., La Bella, A., Puleo, G., Scattolini, R., Rossetti, A., & Sandroni, C. (2019). Modelling and predictive control of a solar cooling plant with flexible configuration. *Journal of Process Control*, *76*, 74–86.

Rawlings, J. B., Mayne, D. Q., & Diehl, M. (2017). *Model predictive control: Theory, computation, and design, vol. 2*. Nob Hill Publishing Madison.

Sandou, G., Font, S., Tebbani, S., Hiret, A., Mondon, C., Tebbani, S., et al. (2005). Predictive control of a complex district heating network. In *IEEE conference on decision and control: Vol. 44*, (8), (p. 7372).

Sarbu, I., Mirza, M., & Crasmareanu, E. (2019). A review of modelling and optimisation techniques for district heating systems. *International Journal of Energy Research*, *43*(13), 6572–6598.

Taylor, M., Long, S., Marjanovic, O., & Parisio, A. (2021). Model predictive control of smart districts with fifth generation heating and cooling networks. *IEEE Transactions on Energy Conversion*, *36*(4), 2659–2669.

Vasilj, J., Gros, S., Jakus, D., & Zanon, M. (2017). Day-ahead scheduling and real-time economic MPC of CHP unit in microgrid with smart buildings. *IEEE Transactions on Smart Grid*, *10*(2), 1992–2001.

Verrilli, F., Parisio, A., & Glielmo, L. (2016). Stochastic model predictive control for optimal energy management of district heating power plants. In *2016 IEEE 55th conference on decision and control* (pp. 807–812). IEEE.

Verrilli, F., Srinivasan, S., Gambino, G., Canelli, M., Himanka, M., Del Vecchio, C., et al. (2016). Model predictive control-based optimal operations of district heating system with thermal energy storage and flexible loads. *IEEE Transactions on Automation Science and Engineering*, *14*(2), 547–557.

Werner, S. (2022). Network configurations for implemented low-temperature district heating. *Energy*, Article 124091.

Wirtz, M., Neumaier, L., Remmen, P., & Müller, D. (2021). Temperature control in 5th generation district heating and cooling networks: An MILP-based operation optimization. *Applied Energy*, *288*, Article 116608.

Zdravković, M., Ćirić, I., & Ignjatović, M. (2022). Explainable heat demand forecasting for the novel control strategies of district heating systems. *Annual Reviews in Control*, *53*, 405–413.